Heliyon 10 (2024) e32513

Contents lists available at ScienceDirect

Heliyon

journal homepage: www.cell.com/heliyon

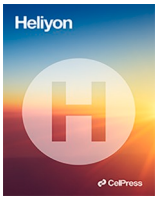

Research article

Precise maxillofacial soft tissue reconstruction: A combination of cone beam computed tomography and 3dMD photogrammetry system

Kaizhao Guo [a,b,c,d,e], Min Li [a,c,d,e], Jiewen Qi [a,c,d,e], Shengyang Han [a,c,d,e], Xiaoshan Wu [a,c,d,e,1,**], Feng Guo [a,e,1,*]

[a] Department of Oral and Maxillofacial Surgery, Xiangya Hospital, Central South University, Changsha, China
[b] Department of Stomatology, Strategic Support Force Medical Center, Beijing, China
[c] Academician Workstation for Oral-Maxillofacial Regenerative Medicine, Central South University, Changsha, China
[d] Research Center of Oral and Maxillofacial Development and Regeneration, Xiangya Hospital, Central South University, Changsha, China
[e] National Clinical Research Center for Geriatric Diseases, Xiangya Hospital, Central South University, Changsha, China

ARTICLE INFO

Keywords:
Soft tissue reconstruction
Maxillofacial surgery
Digital planning
3dMD
CBCT

ABSTRACT

Introduction: The reconstruction of both extra- and intra-oral soft tissue defects, particularly in restoring the morphology of the lip and the corners of the mouth, has posed a significant challenge for surgeons. Inappropriate methods often lead to maxillofacial deformity which then causes psychological and functional problems. This study aimed to address the challenge of reconstructing extensive and complex maxillofacial soft tissue defects, mainly focusing on the lip, the corners of the mouth, and the surrounding areas.

Materials and methods: We developed a reconstruction approach by combining the 3dMDface System (3dMD) with the cone beam computed tomography (CBCT). Firstly, with the extra-oral incision line, we evaluated the shape and the size of the extra-oral defect with 3dMD digitally. Then we used the corresponding maxillary and mandible tooth positions to record the intra-oral defect, which was then converted to digital images by combining 3dMD and CBCT. The islands of the anterolateral thigh perforator flap were then designed after the locations of the perforators were detected with Doppler ultrasonography.

Results: A clinical case diagnosed as dermatofibrosarcoma protuberans was presented to illustrate the approach. The patient's tumor resection and the size of multiple defects were measured and simulated via the virtual surgery system. A three-island perforator flap from the descending branch of the lateral femoral circumflex artery was designed accurately. Two weeks post-operatively, the flap was healed as anticipated and the patient was satisfied with the profile.

Conclusion: The combination of the 3dMD and CBCT technologies improves the accuracy and fitness of extra- and intra-oral soft tissue reconstruction.

* Corresponding author. Department of Oral and Maxillofacial Surgery, Xiangya Hospital, Central South University, Xiangya Road 87#, Changsha, 410008, China.
** Corresponding author. Department of Oral and Maxillofacial Surgery, Xiangya Hospital, Central South University, Xiangya Road 87#, Changsha, 410008, China.
E-mail addresses: drwuxiaoshan@csu.edu.cn (X. Wu), dentguo@126.com (F. Guo).
[1] The two authors contributed equally as corresponding authors

https://doi.org/10.1016/j.heliyon.2024.e32513
Received 3 January 2024; Received in revised form 2 April 2024; Accepted 5 June 2024
Available online 7 June 2024

1. Introduction

Defects affecting multiple regions in oral and maxillofacial tissue present a prevalent challenge for practitioners in the field of oral and maxillofacial surgery [1]. Due to the complex anatomical structure and function of the head and neck region, these defects, characterized by apparent irregularities and asymmetry, are particularly difficult to address [2]. Appropriate reconstruction is of critical importance for aesthetics and maintaining essential functions [3]. Deficiencies caused by inappropriate reconstruction may result in functional issues with chewing, swallowing, speech, and breathing, consequently leading to psychological problems including diminished self-esteem, anxiety, and depression [4].

In clinical practice, various methods are commonly used for soft tissue reconstruction, including free or pedicled flaps, prostheses, skin grafts, and biocompatible polymer-based materials [5–7]. For large-area and multi-site soft tissue defects, the use of free vascularized flap has become one of the most reliable and versatile options [8]. Moreover, with the advancements in digital technology, perforator flaps can now be meticulously designed as branched structures, offering enhanced flexibility and precision [9]. The challenge for clinicians now lies in integrating various technologies to address the diverse and ever-evolving surgical needs. For example, the 3dMDface System (3dMD) is renowned for its exceptional precision in capturing highly detailed three-dimensional images of human subjects. Unlike CT soft tissue reconstruction model, 3dMD offers distinct advantages, including enhanced surface detail, accurate texture, color reproduction, radiation-free imaging, and comprehensive visualization [10,11]. Its compatibility with cone-beam computed tomography (CBCT) further enhances its utility, allowing for comprehensive assessment of both surface and volumetric imaging. This integration facilitates precise treatment planning in complex cases like reconstruction surgery, orthognathic surgery and dental implant placement [12].

When addressing soft tissue defects impacting both extra- and intra-oral regions, clinicians face a significant challenge in accurately designing the branched flaps [13]. One particular challenge arises in cases involving the corners of the mouth, where reconstructing the morphology of the lips and the corners of the mouth is especially difficult [14]. In this study, we aimed to address this challenge. We designed a novel approach in which the number, shape, and size of skin islands of perforator flaps were designed precisely by combining the 3dMD with CBCT. To illustrate the implementation of this approach, we presented a case of maxillofacial dermatofibrosarcoma with multiple masses and evaluated the postoperative reconstruction outcomes.

2. Materials and methods

2.1. Study design and setting

The study was authorized and conducted by the Department of Oral and Maxillofacial Surgery, Xiangya Hospital, Central South University, Changsha, Hunan province, China. It aimed to introduce a new approach that combines 3dMD with CBCT technology for digitally designing the reconstruction of both extra- and intra-oral soft tissue defects. A clinical case was presented to illustrate the approach. The study received approval from the Medical Ethics Committee of Xiangya Hospital, Central South University (approval no. 202201016). Consent was obtained for experimentation with human subjects. The privacy rights of human subjects were observed.

2.2. Participants

This approach is applicable for cases involving both extra- and intra-oral soft tissue defects, particularly those that affect the corners of the mouth. The patients' demographics, including age, sex, pathology, lip defect, size of extra- and intra-oral soft tissue defects, number of flap islands, size of flap islands, donor site position, long-term complications, follow-up time, and status, are considered (Table 1).

The inclusion criteria comprised: 1) Patients with extra- and intra-oral defects of maxillofacial soft tissue without any obvious bone defects after resection. Extra-oral soft tissue defects may include those in the frontofacial region, orbital region, nasal region, infraorbital region, zygomatic region, buccal region or lip region. 2) The size of the donor site should be sufficient to meet the

Table 1
Patient demographics.

Age/Sex	Pathology	Lip Defect	Extra-oral Defect Size (cm^2) *	Intra-oral Defect Size (cm^2) *	Number of Flap Islands	Size of Flap Islands (cm^2) *	Donor Site Position	Long-term Complications	Follow-up (months)	Status
45/ Male	Dermatofibrosarcoma protuberans	Upper lip & right corner of the mouth	64.67	22.34	3	Island 1 15.67 Island 2 49.00 Island 3 22.34	Anterolateral thigh	Ectropion**	24	Alive without relapse

*All data were obtained with preoperative simulation.
* The ectropion was due to the post-operative radiotherapy and did not appear within the first six months after the surgery.

requirements for reconstruction. Specifically, the surface area of healthy anterolateral femoral skin should be larger than the defect area. 3) The location of the lateral femoral circumflex artery perforators should align with each designed flap island to ensure a proper match.

The exclusion criteria comprised: 1) Soft tissue defects affected both sides of the oral and maxillofacial region and did not have a mirror symmetry reference. 2) Presence of trauma, scars, color changes, or other deformities in the skin of the donor site. 3) Patients with surgical contraindications, including severe signs and symptoms of peripheral artery disease of the lower extremities. One patient was included in this study. The participant's rights were protected, and informed consent was obtained from the participant for the presentation of this paper and accompanying images.

2.3. Virtual surgical planning

The 3dMD images were recorded using the 3dMDface.t System (3Q Technologies, Atlanta, GA, USA) and analyzed with the image-processing software 3dMDvultus (3dMD, Atlanta, GA, USA). This noninvasive 3D surface scanner employs active stereo-photogrammetry and random infrared speckle projection to capture both pattern-projected and nonpattern-projected white light images simultaneously, capturing at 10 frames per second, with an accuracy of 0.2 mm [11]. The cone-beam CT scans were obtained using a CBCT scanner (KaVo 3D eXam, Germany) with the following properties: 230V, 5A, thickness 0.250 mm, 50/60Hz, and 1150VA.

All of the scans and images were necessary for diagnosis and treatment planning, and were taken by experienced doctors. The CBCT data were stored in DICOM format, and the 3dMD data were stored in BMP format. The measurements and analysis of both formats were directly processed into the image-processing software 3dMDvultus. And Rhinoceros 3D (Robert McNeel and Associates for Windows, Washington DC, USA) was used to planarize the flap model.

Firstly, we marked the extra-oral incision line 5 mm outside the tumor boundary. Then 3DMD and CBCT examinations were performed on the patient. The shape, size, and curve of the extra-oral defect were evaluated using the 3dMDface.t System digitally, by mirroring the other side (Fig. 1A). To evaluate the intra-oral defect, we marked the incision margin by recording the positions of the corresponding maxillary and mandible teeth, which were located 5 mm outside the tumor boundary. The intra-oral defect was then evaluated and converted into digital images by combining the 3dMD and CBCT files (Fig. 1B). The virtual surgical schematic (Fig. 1) was based on the author's actual photos and images, and has been authorized and agreed upon.

The defects were reconstructed using multiple islands of perforator flap sourced from the descending branch of the lateral femoral circumflex artery. The curve surface of the reconstructed flap islands was transformed into a plane using Rhinoceros 3D software. Subsequently, the morphology of the flap islands was printed at a 1:1 ratio using 3D printing technology. Doppler ultrasonography was then used to accurately locate the perforators at the donor site. Finally, the design was completed by placing the printed models of flap islands on the donor site.

The step-by-step protocols of virtual surgical planning can be summarized below: 1) mark the boundary of defects; 2) take 3dMD and CBCT; 3) evaluate the extra-oral defect; 4) segment extra-oral defect (if necessary); 5) mirror the other side over; 6) design extra-oral flap island models; 7) locate intra-oral incision margin; 8) evaluate the intra-oral defect; 9) design intra-oral flap island models; 10) planarize the flap island models; 11) print the flap island models; 12) choose donor site; 13) take doppler ultrasonography; 14) design flap island locations.

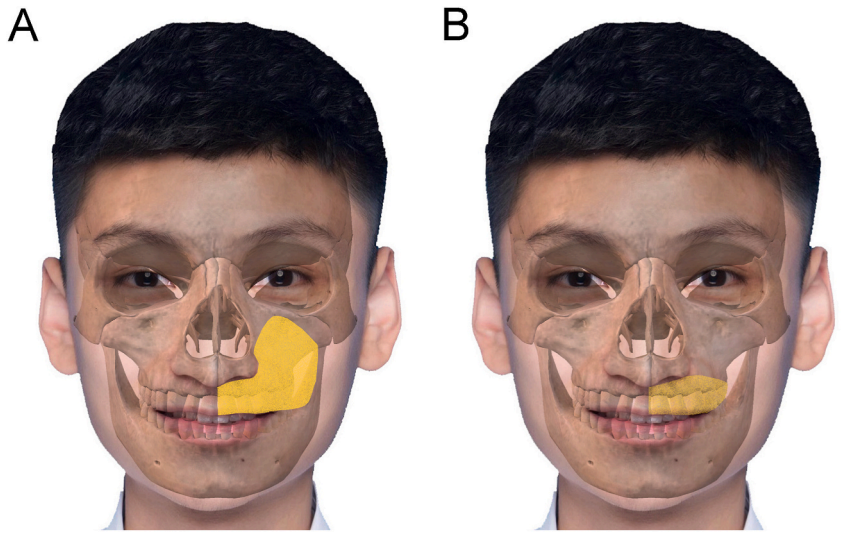

Fig. 1. The extra- and intra-oral flap islands were designed by the combination of 3dMD and CBCT digitally.
(1A) Yellow area shows the size and shape of the extra-oral flap**. (1B)** Yellow area shows the size and shape of the intra-oral flap.

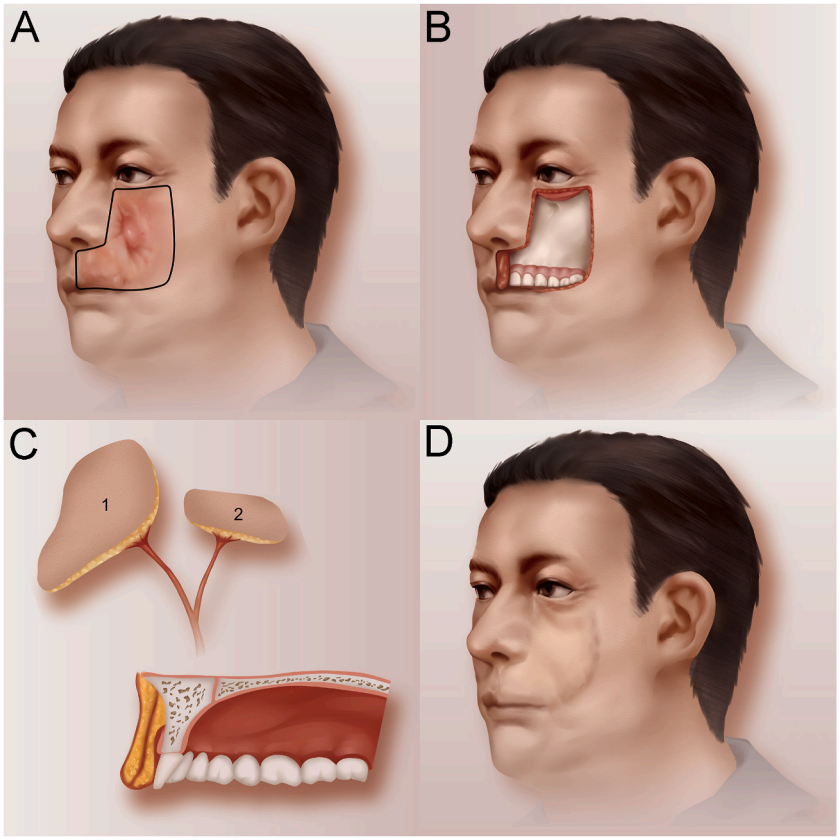

Fig. 2. The Surgical method diagram.
(2A) The resection range was marked 5 mm outside the tumor boundary. **(2B)** Weber-Ferguson incision was used for enlarged tumor excision. **(2C)** The ALTPs were harvested for extra- and intra-oral reconstruction. **(2D)** Expected postoperative recovery.

2.4. Surgical techniques

The Weber-Ferguson incision was used for enlarged tumor excision (Fig. 2A–B). The anterolateral thigh perforator flap (ALTP) was chosen for the reconstruction after radical resection.

The ALTP harvesting method was previously described [8]. In summary, prior to surgery, the perforators were marked and the shape of the flap islands was drawn on the anterolateral thigh region. During surgery, the perforators were dissected retrogradely to the descending branch of the lateral circumflex femoral artery (LCFA), while maintaining the integrity of the fascia lata. The branch artery and vein of the LCFA were then anastomosed with the facial artery and vein to reconstruct the defect region. Each flap island was placed according to the preoperative design to restore the morphology and three-dimensional aesthetic contour of the soft tissue. Flap Island 1 was used for the reconstruction of the extra-oral soft tissue defect, while Flap Island 2 was used to restore the intra-oral lip and buccal mucosa (Fig. 2C–D).

2.5. Follow-up

A two-year follow-up was planned before surgery. After discharge, the patient would be followed up monthly in the first six months, and every six months thereafter. Besides, the physical examination, evaluation of complications, psychology status and appearance would be carried out every time the patient came for visit.

2.6. Effect evaluation

Following the surgery, 3dMD scans were utilized to evaluate the aesthetic and symmetry of the oral and maxillofacial region morphology upon the patient's discharge. To conduct a quantitative analysis, we selected five indices: nasolabial angle, total upper lip height, length of the right upper lip, length of the left upper lip, and mouth width. In 2016, Jodi Caple and Carl N. Stephan proposed a standardized nomenclature for craniofacial and facial anthropometry [15]. And we providing the explanation of each index below, all landmarks are soft tissue marks.

Nasolabial angle refers to the angulation calculated from intersecting lines drawn from the Pronasale point to the Subnasale point

and from the Labial superius point to the Subnasale point. The Pronasale point is the most anteriorly protruded point of the apex nasi. The Subnasale point is the median point at the junction between the lower border of the nasal septum and the philtrum area. The Labial superius point is the midpoint of the vermilion border of the upper lip.

Total upper lip height is the linear distance between the Subnasale point and the Stomion point. The Stomion point is the midline point of the labial fssure when the lips are naturally closed, with teeth shut in the natural position. If the Stomion point is not in the midline, it is located below the philtrum. Length of the upper lip (right and left) is the linear distance between the Labial superius point and the Cheilion point. The Cheilion point is a bilateral point and represents the outer corners of the mouth where the outer edges of the upper and lower vermilions meet. Mouth width refers to the linear distance between the two sides of the Cheilion points.

2.7. Quality control and statistics

All researchers underwent the same training and followed identical measurement standards. Two researchers, unaware of the group information, independently conducted three measurements for each case. The deviations of quantitative indices before and after surgery were then calculated.

3. Results

3.1. Clinical case

A case in May 2021 was selected to illustrate the design protocol and implementation. The patient, a 45-year-old male, was diagnosed with maxillofacial dermatofibrosarcoma protuberans at Xiangya Hospital of Central South University (Fig. 3A–C). Ten years ago, a mass was discovered in the infraorbital region and was surgically removed without undergoing a pathological examination at a local hospital. Five years later, the tumor recurred and grew larger in its original location, which was surgically removed at the local hospital. Following the secondary resection, the defect was covered using a free skin graft. The postoperative pathological diagnosis confirmed 'dermatofibrosarcoma protuberans'. Over the past two years, the tumor recurred for the second time, and its growth rate accelerated. Multiple areas, including the superciliary arch, nasal dorsum, inner canthus, infraorbital, zygomatic, buccal, and intra-oral buccal and lip mucosa regions, have been affected. Intra-oral examination revealed significant swelling of the right upper lip and buccal mucosa, along with multiple hard masses extending from facial tumors (Fig. 3 D). The orifice of the parotid duct remained unaffected (Fig. 3E). Pathology consultation, magnetic resonance imaging (MRI), CBCT, and positron emission tomography-computed tomography (PET-CT) examinations were conducted at our hospital, confirming the presence of multiple masses in the skin, mucosa, and subcutaneous tissues (Fig. 3F–J).

3.2. Digital design for reconstruction of extra- and intra-oral defects

The preparation of the therapeutic schedule involved several steps. First, the tumor boundary was determined through palpation, combining imagological examination and marked with a black marker pen (Fig. 3A). The teeth positions corresponding to the intra-oral resection margin were recorded (Fig. 3 D). Then, a three-dimensional profile was created digitally using the 3dMDface System and the image-processing software 3dMDvultus (Fig. 4A). The extra-oral resection margin was marked 5 mm outside the tumor boundary digitally with a red line. To reconstruct this marked area, the other side was digitally mirrored to match the defect area. The extra-oral area was large and had an irregular shape, making it difficult to harvest one flap island to complete the reconstruction. Therefore, we separated it into two areas (Area 1st: 15.669 cm^2, volume: 2.761 cc; Area 2nd: 49.000 cm^2, volume: 20.045 cc) to facilitate the harvesting of a multiple-island perforator flap (Fig. 4 B–C).

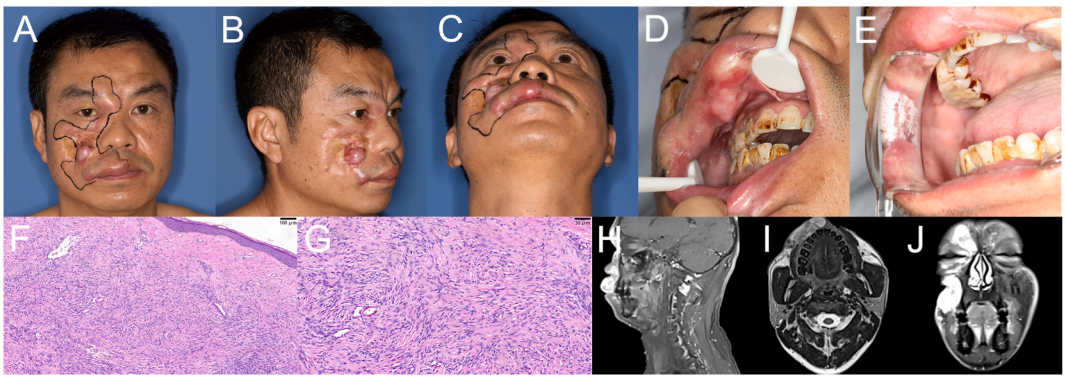

Fig. 3. Preoperative examination of the patient.
(3A-C) Tumors and the ranges marked by lines. **(3D-E)** Intra-oral examination. **(3F)** Pathological diagnosis in 20 × . **(3G)** Pathological diagnosis in 40 × . **(3H-J)** MRI images.

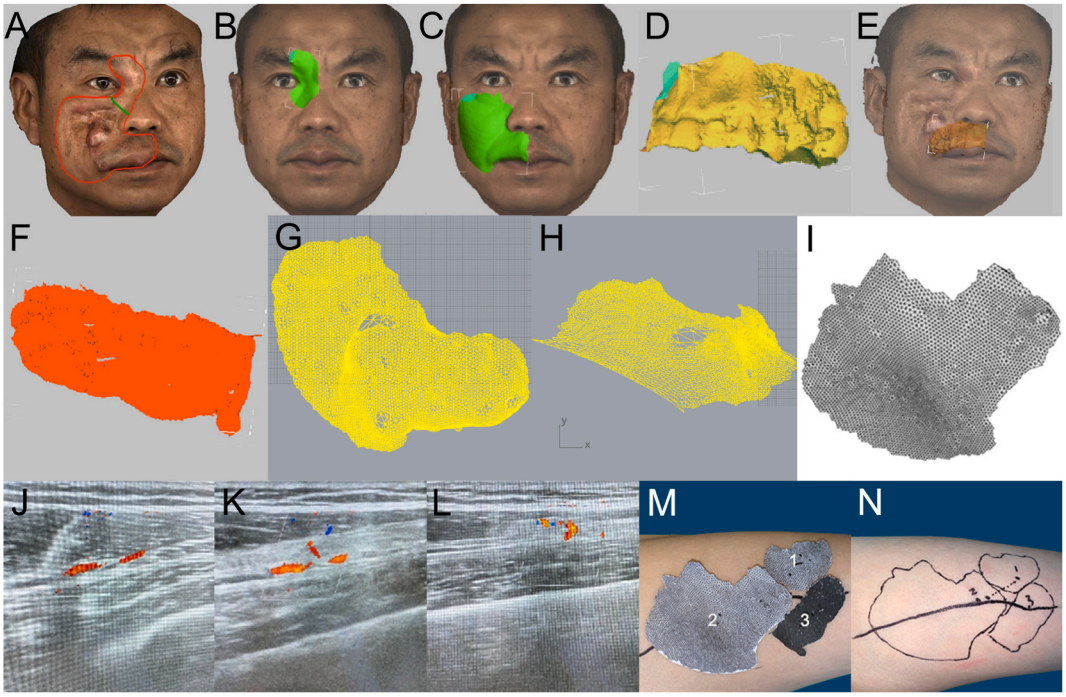

Fig. 4. Digital simulation and reconstruction design.
(4A) Three-dimensional profile made with the 3dMDface System digitally; excision margin was marked with red line; the extra-oral defect was separated into 2 areas. **(4B)** The shape of flap island 1. **(4C)**: The shape of flap island 2. **(4D-E)** CBCT image was projected to 3dMD image to design the intra-oral flap. **(4F)** The shape of the intra-oral defect region.
(4G-H) The curved surface of the flap island 2 was expanded into a plane. **(4I)** The flap island 2 was printed in a 1:1 ratio. **(4J-L)** Three perforators from the descending branch were located on the anterolateral thigh region with the use of color Doppler flow imaging. **(4M-N)** The flap islands were printed and mapped on the anterior thigh to design the three-island perforator flap.

To facilitate the reconstruction of the intra-oral lip and buccal mucosa, CBCT images were used in conjunction with 3dMD images to simulate the size and shape of the intra-oral defect. Based on the palpation and imagological examination, it was recommended to resect the lip and buccal mucosa from the distal plane of the maxillary right first molar to the distal plane of the maxillary left central incisor.

The upper boundary of the intra-oral defect was set 3–4 mm above the root apex of the maxillary right permanent canine, running

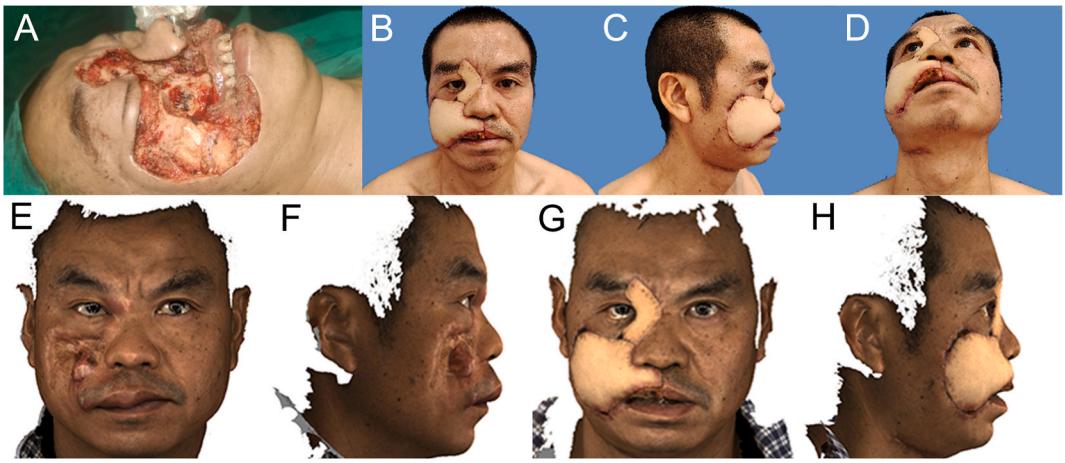

Fig. 5. Intraoperative and postoperative images of the patient.
(5A) The tumors were removed to the bone surface. (5B-D) Postoperative photographs of the patient when hospital discharge. (5E) Front 3dMD image before surgery. (5F) Side 3dMD image before surgery. (5G) Front 3dMD image when hospital discharge. (5H) Side 3dMD image when hospital discharge.

parallel to the vermilion border. This was done to reconstruct the maxillary vestibule groove. The lower boundary was set according to the left (unaffected side) corner of the mouth, parallel to the curve of occlusion, in order to reconstruct the transition between the vermilion and inner lip mucosa. Further minor adjustments were made to ultimately determine the intra-oral defect (Area 3rd: 22.343 cm^2, volume 6.798 cc) (Fig. 4D–F).

3.3. Digital design for perforator flap islands

Then a three-island perforator flap was designed from the descending branch of the lateral femoral circumflex artery according to the three areas identified above. The curved surfaces of the three areas were transformed into planes using Rhinoceros 3D software and printed in a 1:1 ratio (Fig. 4G–I). Prior to the surgery, the three perforators of the descending branch were located on the anterolateral thigh region with the assistance of Doppler ultrasonography (Fig. 4J–L). The printed areas were then mapped onto the anterolateral thigh region to determine the size and area of the three islands of the flap (Fig. 4M–N).

3.4. Surgical procedure and follow-up

The surgery began with the removal of the tumors, which were completely excised down to the bone surface (Fig. 5A). We then proceeded to harvest a three-island perforator flap from the descending branch of the lateral femoral circumflex artery (LCFA). Flap Island 1 was used for reconstructing the superciliary arch, nasal dorsum, and inner canthus. Flap Island 2 was used for reconstructing the infraorbital, zygomatic, and buccal regions. Flap Island 3 was used for restoring the intra-oral lip and buccal mucosa. During the operation, the artery and vein of the descending branch of the lateral femoral circumflex artery were anastomosed with the facial artery and vein. The extensive and complex maxillofacial soft tissue defects were successfully covered, resulting in accurate and smooth reconstruction. The patient was satisfied with the postoperative appearance.

Postoperative observation and care revealed that the flap had a satisfactory blood supply with no occurrence of complications. The patient achieved an aesthetically pleasing facial profile (Fig. 5B–D). Two weeks after the surgery, the patient was discharged and subsequently followed up monthly for the first six months and every six months thereafter. During each visit, a physical examination, evaluation of complications, assessment of psychological status, and evaluation of appearance were conducted. The postoperative pathological diagnosis was 'maxillofacial dermatofibrosarcoma protuberans'. After the initial six months, the patient requested to return to his hometown and underwent a course of radiation therapy (200.0 cGy each time for 30 sessions) at the local hospital. Six months later, during his follow-up visit, the patient developed ectropion as a result of the radiation therapy. Over the next year, the patient was followed up every three months. There was no disease recurrence, and the condition of the eyelids improved.

3.5. Effect evaluation

The morphology of the aesthetic and symmetry of reconstruction was assessed by measuring the nasolabial angle, total upper lip height, length of the right upper lip, length of the left upper lip, and mouth width. A comparison was made between the preoperative and postoperative data of the patient (Table 2, Fig. 5E–H). The results showed that the nasolabial angle increased by 5°. Following the resection and reconstruction of the tumor, the total upper lip height decreased by 0.8 cm, the mouth width also decreased by 0.3 cm, and the lengths of the right and left upper lip became equal.

4. Discussion

The precision reconstruction of oral and maxillofacial defects is emerging as a trend. Surgeons are striving to achieve a seamless integration of aesthetic and functional recovery by accurately reconstructing the affected area. Extensive research and application of digital reconstruction techniques have been focused on hard tissues, such as teeth and bones [16]. For instance, CBCT can accurately simulate hard tissue structures, facilitating more precise assessments of bone volume, density, and other critical parameters [17]. Three-dimensional printing technology can be utilized to create personalized models of teeth and bones, either for pre-surgical planning or as direct implant materials [18]. In contrast, research on digital reconstruction of soft tissues remains limited. While 3dMD serves as an advanced facial scanning instrument capable of simulating facial soft tissue morphology, it provides a relatively accurate assessment of key soft tissue parameters such as area and volume [11]. The challenge for clinicians now lies in integrating

Table 2
Effective evaluation of the morphology after reconstruction.

	Nasolabial angle	Total upper lip height	Length of The Right Upper Lip	Length of The Left Upper Lip	Mouth width
Pre-operation	104°	2.8 cm	3.0 cm	2.7 cm	5.3 cm
Post-operation	109°	2.0 cm	2.7 cm	2.7 cm	5.0 cm
Deviation	+5°	−0.8 cm	−0.3 cm	0	0.3 cm

*All data were evaluated by the 3dMD images.
**All landmarks were soft tissue marks.
***All researchers underwent the same training and followed identical measurement standards. Two researchers, unaware of the group information, independently conducted three measurements for each case.

various technologies to meet the diverse and evolving surgical needs.

The three-dimensional nature of the oral and maxillofacial region presents a significant challenge for soft tissue reconstruction. In clinical practice, various approaches such as soft tissue flaps, prostheses, skin grafts, composite free flaps, and biocompatible polymer-based materials are commonly used [10,19]. Currently, biocompatible polymer skin implants play a crucial role in reconstructing soft tissue defects in the maxillofacial region. Their versatility allows for application in various soft tissue reconstruction procedures, including those for facial trauma, tumor resection, and congenital deformities [20,21]. However, when confronted with extensive defects affecting both extra- and intra-oral regions, they lack sufficient tissue attachment and are therefore not suitable. Traditional perforator flaps, which are designed and manipulated by surgeons based on the defect area and shape, may require additional trimming before reconstruction. Consequently, although traditional perforator flaps may adequately cover the defect, the functionality and appearance may not always be optimal [22]. To overcome this issue, we employed a mirror symmetry approach by 3dMD to virtually reconstruct the ideal three-dimensional structure of the defected area. Utilizing this model, we can accurately measure the area and volume, thereby facilitating planarized printing to tackle this intricate challenge.

Reconstruction surgeons have long faced the challenge of treating combined extra- and intra-oral defects, especially in restoring the morphology of the lips and the corners of the mouth [7,23,24]. Smaller defects can be addressed with local flap transfers, larger areas necessitate the use of prostheses or free flaps [5,6]. While 3D-printed prostheses, when combined with digital design, have demonstrated potential in restoring facial aesthetics, free flaps for soft tissue reconstruction offer advantages in tissue mobility and comfort. However, using free flaps for reconstructing large and intricate defects also requires careful consideration of the flap design and the donor site selection [25]. In our innovative approach, we have utilized a combination of 3dMD and CBCT technologies to create a unified digital reconstruction design for the corners of the mouth. The 3dMD technology allows us to plan the excision scope in advance, while the integration of CBCT provides us with a three-dimensional structure and volume of the defect area, thereby facilitating accurate flap design. Especially, the reconstruction of the lip's morphological shape, taking into account both soft and hard tissue factors with the assistance of CBCT, is crucial in ensuring the desired facial appearance post-surgery.

The nasolabial angle, as well as the length and height of the lip, are commonly used as aesthetic evaluation indicators following nasolabial reconstructive surgery [26–28]. In this case, the tumor led to swelling and protrusion of the upper lip, causing a decrease in the nasolabial angle and asymmetry between the left and right sides. Following the removal of the tumor and the subsequent reconstruction of the defect, the patient's lip deficiencies were corrected, the nasolabial angle increased, the height of upper lip decrease, and symmetry was restored to the upper lip. While the deviations may not be statistically significant, they hold clinical significance.

Despite the effective reconstruction of patients' facial morphology through this method, it is important to discuss its limitations and explore further directions. Firstly, due to the limited sample size, there may still be more potential risks and challenges that need to be addressed in future studies. A larger patient cohort is needed to validate the custom reconstruction approach. Additionally, this method is unsuitable for patients with bilateral involvement, as it lacks a mirror reference. In such cases, facial transplantation has been proposed as a viable alternative for individuals with extensive bilateral facial involvement. Moreover, patients with malignant tumors may require postoperative radiotherapy, potentially leading to flap atrophy and malnutrition. Although we attempted to avoid the involvement of the eyelids in our design, oncology consultations indicated the necessity of postoperative radiotherapy, ultimately resulting in the development of ectropion. Furthermore, the appearance could be further improved if we take consideration of the thickness, elasticity, and plasticity of the flap. The intrinsic thickness of the flap plays a critical role in its long-term survival and may impact the postoperative appearance. The combination of 3dMD and CBCT provides us with the tissue thickness of the defect area. Further measuring the subcutaneous thickness of the donor skin by ultrasonography may help us select the optimal donor site. However, considering the elasticity characteristics of soft tissues requires a comprehensive approach that combines preoperative imaging, patient-specific modeling, biomechanical analysis, intraoperative assessment, and surgical expertise.

In the future, we plan to continue integrating the applications of 3dMD and CBCT to enhance surgical planning and outcomes. By combining these technologies, we hope to refine patient-specific modeling and biomechanical analysis, thereby enabling us to design perforator flaps with improved flexibility and accuracy. These will allow us to determine the precise shape, size, and thickness of the defect areas and match them with the flaps, thereby optimizing surgical outcomes. We firmly believe that the combination of 3dMD photogrammetry and CBCT scans provides a highly accurate and innovative approach for reconstructing extensive and complex defects in oral and maxillofacial surgery, demonstrating excellent fitness and feasibility.

5. Conclusion

The combination of 3dMD and CBCT technologies enhances the accuracy and fitness of extra- and intra-oral soft tissue defect reconstruction. This approach shows potential for advancements in oral and maxillofacial surgery, improving functionality and aesthetics through digital planning and personalized flap design.

Ethics approval and consent to participate

The Medical Ethics Committee of Xiangya Hospital, Central South University, approved this study. The reference number is 202201016. Consent was obtained for experimentation with human subjects. The privacy rights of human subjects were observed. The work described has been carried out in accordance with The Code of Ethics of the World Medical Association (Declaration of Helsinki). The participant's rights were protected, and informed consent was obtained from the participant for the presentation of this paper and accompanying images.

Consent for publication

Not applicable.

Funding

This research did not receive any specific grant from funding agencies in the public, commercial, or not-for-profit sectors.

Data availability statement

The data generated during the current study are available from the corresponding author upon reasonable request. The data are not publicly available due to privacy or ethical restrictions.

CRediT authorship contribution statement

Kaizhao Guo: Writing – review & editing, Writing – original draft, Visualization, Software, Methodology, Investigation, Formal analysis, Data curation. **Min Li:** Writing – review & editing, Methodology, Data curation. **Jiewen Qi:** Writing – review & editing, Formal analysis, Data curation. **Shengyang Han:** Data curation. **Xiaoshan Wu:** Writing – review & editing, Project administration, Conceptualization. **Feng Guo:** Writing – review & editing, Project administration, Conceptualization.

Declaration of competing interest

The authors declare that they have no known competing financial interests or personal relationships that could have appeared to influence the work reported in this paper.

References

[1] J. Vranckx, O. Desmet, M. Bila, W. Wittesaele, N. Wilssens, V. Poorten, Maxillomandibular reconstruction using insourced virtual surgical planning and homemade CAD/CAM: a single-center evolution in 75 patients, Plast. Reconstr. Surg. 152 (1) (2023) 143e–154e, https://doi.org/10.1097/prs.0000000000010142.
[2] G. Salzano, F. Maffia, L. Vaira, et al., Locoregional flaps for the reconstruction of midface skin defects: a collection of key surgical techniques, J. Clin. Med. 12 (11) (2023), https://doi.org/10.3390/jcm12113700.
[3] R. Cannon, J. Houlton, E. Mendez, N. Futran, Methods to reduce postoperative surgical site infections after head and neck oncology surgery, Lancet Oncol. 18 (7) (2017) e405–e413, https://doi.org/10.1016/s1470-2045(17)30375-3.
[4] A. Sahovaler, D. Yeh, J. Yoo, Primary facial reanimation in head and neck cancer, Oral Oncol. 74 (2017) 171–180, https://doi.org/10.1016/j.oraloncology.2017.08.013.
[5] M. Scaglioni, M. Meroni, E. Fritsche, G. Rajan, Superficial circumflex iliac artery perforator flap in advanced head and neck reconstruction: from simple to its chimeric patterns and clinical experience with 22 cases, Plast. Reconstr. Surg. 149 (3) (2022) 721–730, https://doi.org/10.1097/prs.0000000000008878.
[6] G. Mannelli, L. Gazzini, L. Comini, et al., Double free flaps in oral cavity and oropharynx reconstruction: systematic review, indications and limits, Oral Oncol. 104 (2020) 104637, https://doi.org/10.1016/j.oraloncology.2020.104637.
[7] A. Slijepcevic, A. Afshari, A. Vitale, S. Couch, L. Jeanpierre, J. Chi, A contemporary review of the role of facial prostheses in complex facial reconstruction, Plast. Reconstr. Surg. 151 (2) (2023) 288e–298e, https://doi.org/10.1097/prs.0000000000009856.
[8] R. Yang, X. Wu, P. Kumar, et al., Application of chimerical ALT perforator flap with vastus lateralis muscle mass for the reconstruction of oral and submandibular defects after radical resection of tongue carcinoma: a retrospective cohort study, BMC Oral Health 20 (1) (2020) 94, https://doi.org/10.1186/s12903-020-01066-x.
[9] S. Nyirjesy, M. Heller, N. von Windheim, et al., The role of computer aided design/computer assisted manufacturing (CAD/CAM) and 3- dimensional printing in head and neck oncologic surgery: a review and future directions, Oral Oncol. 132 (2022) 105976, https://doi.org/10.1016/j.oraloncology.2022.105976.
[10] H. Hong, J. Zhou, Q. Fan, et al., Characteristics of spatial changes in molars and alveolar bone resorption among patients with loss of mandibular first molars: a CBCT-based morphometric study, J. Clin. Med. 12 (5) (2023), https://doi.org/10.3390/jcm12051932.
[11] Z. Xue, L. Wu, T. Qiu, Z. Li, X. Wang, X. Liu, Three-dimensional dynamic analysis of the facial movement symmetry of skeletal class III patients with facial asymmetry, J. Oral Maxillofac. Surg. : official journal of the American Association of Oral and Maxillofacial Surgeons 78 (2) (2020) 267–274, https://doi.org/10.1016/j.joms.2019.09.007.
[12] J. Moratin, J. Mrosek, D. Horn, et al., Full-thickness tumor resection of oral cancer involving the facial skin-microsurgical reconstruction of extensive defects after radical treatment of advanced squamous cell carcinoma, Cancers 13 (9) (2021), https://doi.org/10.3390/cancers13092122.
[13] D. Deng, J. Liu, F. Chen, et al., Double-island anterolateral thigh free flap used in reconstruction for salvage surgery for locally recurrent head and neck carcinoma, Medicine 97 (41) (2018) e12839, https://doi.org/10.1097/md.0000000000012839.
[14] X. Gao, K. Tian, L. Huang, et al., Introducing the thin and ultrathin submental artery perforator flaps for precise reconstruction following T1-2 oral cavity cancer resection, Oral Oncol. 135 (2022) 106234, https://doi.org/10.1016/j.oraloncology.2022.106234.
[15] J. Caple, C. Stephan, A standardized nomenclature for craniofacial and facial anthropometry, Int. J. Leg. Med. 130 (3) (2016) 863–879, https://doi.org/10.1007/s00414-015-1292-1.
[16] H. Nakano, K. Suzuki, K. Inoue, et al., Application of the homologous modeling technique for precision medicine in the field of oral and maxillofacial surgery, J. Personalized Med. 12 (11) (2022), https://doi.org/10.3390/jpm12111831.
[17] D. Annino, E. Hansen, R. Sethi, et al., Accuracy and outcomes of virtual surgical planning and 3D-printed guides for osseous free flap reconstruction of mandibular osteoradionecrosis, Oral Oncol. 135 (2022) 106239, https://doi.org/10.1016/j.oraloncology.2022.106239.
[18] T. Chan, C. Long, E. Wang, E. Prisman, The state of virtual surgical planning in maxillary Reconstruction: a systematic review, Oral Oncol. 133 (2022) 106058, https://doi.org/10.1016/j.oraloncology.2022.106058.
[19] D. Gunawardena, D. Howes, S. Fleming, et al., Reconstruction of a maxillectomy and rhinectomy defect utilising a novel subperiosteal prosthesis and magnet-retained nasal prosthesis: a case report, Oral Oncol. 135 (2022) 106222, https://doi.org/10.1016/j.oraloncology.2022.106222.
[20] M. Gholipourmalekabadi, S. Sapru, A. Samadikuchaksaraei, R.L. Reis, D.L. Kaplan, S.C. Kundu, Silk fibroin for skin injury repair: where do things stand? Adv. Drug Deliv. Rev. 153 (2020 Jan 1) 28–53, https://doi.org/10.1016/j.addr.2019.09.003.

[21] P. Yudaev, V. Chuev, B. Klyukin, A. Kuskov, Y. Mezhuev, E. Chistyakov, Polymeric dental nanomaterials: antimicrobial action, Polymers 14 (5) (2022 Feb 22) 864, https://doi.org/10.3390/polym14050864.
[22] W. Yang, W. Choi, M. Wong, et al., Three-dimensionally printed patient-specific surgical plates increase accuracy of oncologic head and neck reconstruction versus conventional surgical plates: a comparative study, Ann. Surg Oncol. 28 (1) (2021) 363–375, https://doi.org/10.1245/s10434-020-08732-y.
[23] I. Tsuge, H. Yamanaka, M. Katsube, Y. Sowa, M. Sakamoto, N. Morimoto, Lower lip reconstruction using a sensory anterolateral thigh flap as the first choice, Plastic and reconstructive surgery Global open 11 (5) (2023) e5003, https://doi.org/10.1097/gox.0000000000005003.
[24] S. Park, K. Lee, Use of super-thin superficial circumflex iliac artery perforator flap for reconstruction of lower lip defect, Plast. Reconstr. Surg. (2023), https://doi.org/10.1097/prs.0000000000010978.
[25] P. Padilla, A. Mericli, R. Largo, P. Garvey, Computer-Aided design and manufacturing versus conventional surgical planning for head and neck reconstruction: a systematic review and meta-analysis, Plast. Reconstr. Surg. 148 (1) (2021) 183–192, https://doi.org/10.1097/prs.0000000000008085.
[26] T. Nayak, K. Bonanthaya, R. Parmar, P. Shetty, Long-term comparison of the aesthetic outcomes between nasoalveolar molding- and non-nasoalveolar molding-treated patients with unilateral cleft lip and palate, Plast. Reconstr. Surg. 148 (5) (2021) 775e–784e, https://doi.org/10.1097/prs.0000000000008463.
[27] A. Paradowska-Stolarz, B. Kawala, The nasolabial angle among patients with total cleft lip and palate, Adv. Clin. Exp. Med. : official organ Wroclaw Medical University 24 (3) (2015) 481–485, https://doi.org/10.17219/acem/28112.
[28] G. Raschke, U. Rieger, R. Bader, M. Kirschbaum, N. Eckardt, S. Schultze-Mosgau, Evaluation of nasal reconstruction procedures results, Journal of cranio-maxillo-facial surgery 40 (8) (2012) 743–749, https://doi.org/10.1016/j.jcms.2012.01.023, official publication of the European Association for Cranio-Maxillo-Facial Surgery.